

# A NUMERICAL APPROACH FOR DYNAMIC ANALYSIS OF MARINE SYSTEMS

**Leandro Ribeiro dos Santos**

Computational Solids Mechanics Laboratory  
Federal University of Rio de Janeiro, PEM/COPPE.  
P.O. Box 68503, 21945-970, Rio de Janeiro, RJ, Brazil.  
leandro@mecsol.ufrj.br

**Fernando Alves Rochinha**

Computational Solids Mechanics Laboratory  
Federal University of Rio de Janeiro, PEM/COPPE.  
P.O. Box 68503, 21945-970, Rio de Janeiro, RJ, Brazil.  
faro@serv.com.ufrj.br

*Abstract. The dynamics of flexible systems, such as robot manipulators and cables, is becoming increasingly important in engineering. In the present work a Cosserat continuum theory is adopted, in which the geometry of the rod is described by a smooth mapping defining the spatial position of the line of centroids and an orthonormal frame which defines the relative orientation of the cross-section attached to each point of the curve. In order to solve the nonlinear evolution equations resulting from the modeling, a time-stepping numerical algorithm which achieves stable solutions combined with high precision was developed. The aforementioned numerical methodology is used to the analysis of the nonlinear dynamics of undersea cables. In particular, in order to check the performance of the proposed approach, a cable excited dynamically at its upper end is considered.*

*Keywords: nonlinear rods, dynamics, cables, conserving algorithms.*

## 1. Introduction

Recently there has been a great interest in the study of nonlinear dynamics of structures and its applications to a wide variety of engineering problems. A particular field of great engineering interest is the oil exploitation in deep waters, in which marine systems including flexible risers, umbilicals, synthetic ropes, tethers and towed pipelines undergo large deformations which requires non-linear analysis. All those systems are usually modeled as one dimensional structures, often referred to as rods. The objective of the present work is to use a numerical algorithm dedicated to the simulation of the nonlinear dynamics of rods to simulate the dynamical behavior of these structures.

This time-stepping algorithm preserves exactly fundamental constants of the motion, namely the total linear and total angular momentums and, for the Hamiltonian case, the total energy. In the literature, numerical schemes capable of preserving those quantities are known as conserving algorithms. Three main reasons can be pointed out to motivate the use of such algorithms: the role played by those quantities in the physical and mathematical context; the enhanced numerical capabilities of those algorithms and, finally, the conserved quantities often represent qualitative features of the long term dynamics.

## 2. Non linear dynamics of rods

The geometrically exact mechanical model for rods used in this article is briefly summarised in the present section. Firstly, the geometry of the deformation, which includes finite extension, shear, twist and bending, is presented. After the governing equations, namely the balance of linear and angular momenta, and the constitutive equations, as well, are stated.

### 2.1. Kinematics of Deformation

The geometry of the rod is described by a smooth mapping defining the spatial position of the line of centroids  $\mathbf{c}$  and an orthonormal frame which defines the relative orientation of the cross-section attached to each point of  $\mathbf{c}$ . The central hypothesis in classical theories of rods is that each cross-section undergoes rigid body motion, which means that its shape remains the same during the motion. Accordingly, a configuration of the rod is specified by the following mapping

$$\chi(S, t) = \mathbf{r}(S, t) + X_1 \mathbf{d}_1(S, t) + X_2 \mathbf{d}_2(S, t) \quad (1)$$

where  $\mathbf{r}(S, t)$  defines the position of curve  $\mathbf{c}$ , which is parametrized by the arc-length in the undeformed configuration  $S$ ,  $t$  denotes the time,  $X_1$  and  $X_2$  are local coordinates and  $\mathbf{d}_i(S, t)$  ( $i=1,3$ ) are the directors (Antman, 1981). The geometric picture is depicted in Figure (1), where the reference, for which the associated fields are in capital letter, and deformed configurations are presented. The adopted interpretation of a rod viewed as three-dimensional body constituted of a smooth curve which has attached at each point a plane domain (cross-section) can be considered classic and was introduced and detailed in (Love and Reissner). Throughout this paper, bold letters are used to designate vectors. According to (1), the rod's configuration is

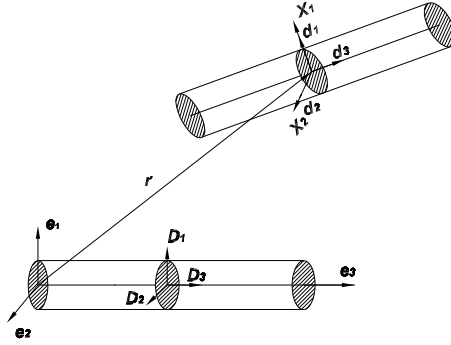


Figure 1: Reference and deformed shapes of structure.

defined by the vector field

$$\Phi = (\mathbf{r}, \mathbf{d}_i) \in \mathbb{K} = V \times K \quad (i = 1, 2, 3) \quad (2)$$

with

$$V = \{\mathbf{r} : [0, L] \rightarrow \mathbb{R}^3 \text{ and appropriate boundary conditions}\}$$

and the nonlinear manifold  $K$  defined by

$$K = \{(\mathbf{d}_1, \mathbf{d}_2, \mathbf{d}_3) : [0, L] \rightarrow \mathbb{R}^9 / \mathbf{d}_i \cdot \mathbf{d}_j = \delta_{ij} \quad (i, j = 1, 2, 3) \text{ and appropriate boundary conditions}\}$$

where  $\delta_{ij}$  is the delta of kronecker and 0 and  $L$  represent the boundary points of the rod. Consequently, one refers to  $\mathbb{K}$  as the abstract configuration manifold of the rod.

**Remark:** Indeed,  $K$  and the special group of rotations  $S0(3)$  can be identified by the isomorphism:

$$\mathbf{d}_i = \mathbf{Q} \mathbf{D}_i \quad (3)$$

where  $\mathbf{Q}$  is a rotation belonging to  $S0(3)$  and  $\mathbf{D}_i$  are the directors in the reference placement ( $t = 0$ ), which, without loss of generality, can be taken coincident with the principal directions of inertia. So, the rotation can be recast as  $\mathbf{Q} = \sum_{i=1}^3 \mathbf{d}_i \otimes \mathbf{D}_i$ , where  $\otimes$  represents the tensorial product.

The usual kinematic boundary conditions consist in:

$$\mathbf{r}(0; L) = \mathbf{r}^{0;L} \quad (\text{rod fixed in the extremity } S = 0 \text{ or } S = L)$$

$$\mathbf{d}_i(0; L) = \mathbf{d}_i^{0;L} \quad \text{for } i \text{ given in } 1, 2, 3 \quad (\text{rod rotating around } \mathbf{d}_i^{0;L} \text{ in the extremities } 0 \text{ or } L)$$

or

$$\mathbf{d}_i(0; L) = \mathbf{d}_i^{0;L} \quad \forall i = 1, 2, 3 \quad (\text{clamped rod in the extremities } 0 \text{ or } L)$$

In fact, it is important, as dynamical situations will be treated, to consider the case where no boundary conditions are prescribed, the so called free boundary or Newman conditions.

Following the kinematical framework presented in Antman, the strain measures of the present theory are given by:  $v_\alpha = \mathbf{r}' \cdot \mathbf{d}_\alpha$  ( $\alpha=1,2$ ) (shear),  $v_3 = \mathbf{r}' \cdot \mathbf{d}_3 - 1$  (extension),  $u_\alpha = \mathbf{u} \cdot \mathbf{d}_\alpha$  ( $\alpha=1,2$ ) (flexion) and  $u_3 = \mathbf{u} \cdot \mathbf{d}_3$  (torsion). Where  $(\ )'$  stands for the partial derivative with respect the arc-length and the vector field  $\mathbf{u}(S, t)$  is defined by the following relation

$$\mathbf{d}_i' = \mathbf{u} \wedge \mathbf{d}_i$$

where  $\wedge$  denotes the ordinary vector product. Unless some reference, throughout subscripts using greek letters are integers ranging from 1 to 2 and those using  $i$  or  $j$  or  $k$  range from 1 to 3.

A motion of the rod is a time dependent curve of configurations denoted by

$$t \in [0, \mathfrak{S}] \rightarrow \Phi_t = (\mathbf{r}_t, \mathbf{d}_{i_t}) \in \mathbb{K} \quad (4)$$

$$\text{with } (\mathbf{r}_t, \mathbf{d}_{i_t}) = (\mathbf{r}(S, t), \mathbf{d}_i(S, t)).$$

According to 4, the velocities and accelerations fields in the present kinematics are

• Translational Motion

$$\mathbf{v} = \dot{\mathbf{r}} \quad ; \quad \mathbf{a} = \dot{\mathbf{v}}$$

• Rotational Motion

$$\dot{\mathbf{d}}_i \quad ; \quad \ddot{\mathbf{d}}_i$$

where  $(\dot{\ })$  stands for the time derivative of  $(\ )$ . The first two fields are the translational velocity and the translational acceleration. The others describe the velocity and acceleration of the angular motion and are related to the angular velocity  $\mathbf{w}$  and the angular acceleration  $\alpha$  of the cross-section by means of :

$$\dot{\mathbf{d}}_i = \mathbf{w} \wedge \mathbf{d}_i \quad (5)$$

$$\ddot{\mathbf{d}}_i = \alpha \wedge \mathbf{d}_i + \mathbf{w} \wedge \dot{\mathbf{d}}_i \quad (6)$$

## 2.2. Local form of the momentum balance equations

The nonlinear system of partial differential equations governing the motion of the rod is constituted by the balance of linear and angular momentum ( Antman, 1981 ), e.g:

$$\mathbf{n}' + \bar{\mathbf{n}} = \bar{\rho} \mathbf{a} \quad (7)$$

$$\mathbf{m}' + \mathbf{r}' \wedge \mathbf{n} + \bar{\mathbf{m}} = I_{22}^\rho (\mathbf{d}_1 \wedge \dot{\mathbf{d}}_1) + I_{11}^\rho (\mathbf{d}_2 \wedge \dot{\mathbf{d}}_2) \quad (8)$$

where  $\mathbf{n}$  and  $\mathbf{m}$  denote the contact resultant force and contact resultant couple per unit of reference arc-length,  $\bar{\mathbf{n}}$  and  $\bar{\mathbf{m}}$  are prescribed body forces and body couples per unit of arc-length acting on the rod,  $\bar{\rho}$  is the mass-density function per unit of reference arc-length which can be interpreted as the average of the three-dimensional density function,  $\rho$ , over the cross section of the rod and  $I^\rho$  is the inertial moment of the mass ( $I_{11}^\rho = \int_A \rho X_2^2 dA$  e  $I_{22}^\rho = \int_A \rho X_1^2 dA$ ). Here,  $A$  denotes the area of the cross-section.

## 3. Variational formulation

In the present section, the system of differential equations formed by ( 7 )-( 8 ) is cast in a variational formulation with the aid of an extended version of the Hamilton's principle introduced by Bayley (1987). This version differs from the classical least action variational principle by the inclusion of an end-point term, yielding

$$\delta \int_{t_1}^{t_2} [J_{kin}(\phi, t) - J_{pot}(\phi, t)] dt - \frac{\partial J_{kin}}{\partial \mathbf{r}} \mathbf{p}|_{t_1}^{t_2} - \sum_{i=1}^3 \frac{\partial J_{kin}}{\partial \mathbf{d}_i} \mathbf{g}_i|_{t_1}^{t_2} = 0, \quad \forall \phi = (\mathbf{r}, \mathbf{d}_k) \in K \quad (9)$$

where  $J_{kin}$  is the kinetic energy of the system and  $J_{pot}$  is the potential energy, which includes both strain energy and the potential of any conservative external forces; like, for instance, forces which are independent of the deformation and motion of the rod. Here  $L = J_{kin} - J_{pot}$  and  $\delta$  denote, respectively, the Lagrangian and the variational operator. Thus, the expression of the variation of kinetic energy is given by

$$\delta J_{kin} = - \int_{t_1}^{t_2} \left[ \int_0^L (\bar{\rho} \mathbf{a} \cdot \mathbf{p} + I_{22}^\rho \ddot{\mathbf{d}}_1 \cdot \mathbf{g}_1 + I_{11}^\rho \ddot{\mathbf{d}}_2 \cdot \mathbf{g}_2) dS \right] dt, \quad \forall \eta = (\mathbf{p}, \mathbf{g}_i) \in dK \quad (10)$$

where  $dK$  is the tangent space at  $K$ , defined by

$$dK = \{(\mathbf{g}_1, \mathbf{g}_2, \mathbf{g}_3) : [0, L] \rightarrow \mathbb{R}^9 / \mathbf{g}_i = \mathbf{U} \wedge \mathbf{d}_i \ \mathbf{U} \in \mathbb{R}^3 \text{ and appropriate boundary conditions}\} \quad (11)$$

and represents the set of admissible variations.

In equation above, it is assumed without loss of generality, that directors are collinear to the principal axis of inertia and that the curve  $c$  is coincident with the line of centroids. One may observe that in this case the translational inertia is completely decoupled from the rotatory inertia, resulting in a similar form to the one of the rigid body dynamics. The expression of the variation of total potential energy is so given by

$$\begin{aligned} \delta J_{pot} = & \int_{t_1}^{t_2} \left\{ \int_0^L \sum_{i=1}^3 \frac{\partial \Psi}{\partial \mathbf{d}_i} \cdot \mathbf{g}_i dS - \int_0^L \bar{\mathbf{n}} \cdot \mathbf{p} dS - \sum_{\alpha=1}^2 \int_0^L \bar{\mathbf{n}}_\alpha \mathbf{g}_\alpha dS + \int_0^L R(\mathbf{r}' - \mathbf{d}_3) \cdot (\mathbf{p}' - \mathbf{g}_3) dS + \right. \\ & \left. + \sum_{i=1}^3 \sum_{j=1}^3 \int_0^L \lambda_{ij} (\mathbf{g}_i \mathbf{d}_j + \mathbf{g}_j \mathbf{d}_i) dS \right\} dt \\ & \forall (\mathbf{p}, \mathbf{g}_i) \in dK \end{aligned} \quad (12)$$

where  $\Psi$  is the elastic energy density, has the following form

$$\Psi(S, \bar{u}, \bar{w}) = \frac{1}{2} (EI_1 \bar{u}_1^2 + EI_2 \bar{u}_2^2 + GJ \bar{u}_3^2)$$

and  $\lambda_{ij}$  are the lagrange multipliers associated to the orthonormality constraint. In equation (12), the effects of shear and extension are introduced via a penalty method. Here, the parameter of penalty  $R$  is adopted equal the axial stiffness of the rod. Besides,  $E$  and  $G$  are interpreted as the Young's modulus and the shear modulus,  $\{I_1, I_2\}$  are the principal moments of inertias and  $J$  is the torsional modulus.

#### 4. Numerical approximation

The numerical treatment of the variational equation (9) is based on a semi-discrete approach involving the spatial discretization through the Finite Element Method and the temporal discretization via the proposed time stepping procedure. The resulting nonlinear algebraic system is solved employing the Newton-Raphson method. The novelty of the proposed approach lies in the treatment of the rotational component of the movement, namely the evolution of the directors.

The functions associated to the translational motion  $(\mathbf{r}, \mathbf{v})$  are discretized by cubic Hermitian finite elements and those associated to the rotational movement  $(\mathbf{d}_i, \dot{\mathbf{d}}_i)$ . Details of the implementation of the finite element discretization can be found in Rochinha (1990), where the static case is addressed.

A numerical evolution scheme consists in given a configuration  $\Phi^n := (\mathbf{r}^n, \mathbf{d}_i^n) \in K$  and its associated velocities  $(\mathbf{v}^n, \dot{\mathbf{d}}_i^n)$ , to obtain the updated configuration  $\Phi^{n+1} := (\mathbf{r}^{n+1}, \mathbf{d}_i^{n+1}) \in K$  and the associated velocities  $(\mathbf{v}^{n+1}, \dot{\mathbf{d}}_i^{n+1})$ , satisfying the governing equations.

Moreover, let  $[t_n, t_{n+1}]$  be a typical interval  $[0, \bar{t}] = U_{n=0}^n [t_n, t_{n+1}]$  and let  $\Delta t = t_{n+1} - t_n$  be the time step interval. The main steps of the proposed algorithm are summarized next.

- Recognize the initial configuration

position:  $\Phi_{(0)}^n := (\mathbf{r}_{(0)}^n, \mathbf{d}_{i(0)}^n) \in K$

velocities:  $(\mathbf{v}_{(0)}^n, \dot{\mathbf{d}}_{i(0)}^n)$

- Step 0: Define a predictor for the translational and rotational fields

• Translation

$$\begin{aligned} \mathbf{r}^{n+1} &= \mathbf{r}^n \\ \mathbf{v}^{n+1} &= -\mathbf{v}^n \end{aligned}$$

• Rotation

$$\mathbf{d}_i^{n+1} = \mathbf{d}_i^n$$

$$\dot{\mathbf{d}}_i^{n+1} = -\dot{\mathbf{d}}_i^n$$

Here, the superscripts  $n$  and  $n+1$  denotes the temporal discrete approximation of a time-varying quantity at time  $t_n$  and  $t_{n+1}$  respectively.

- Step 1: Compute the lagrange multipliers  $\lambda_{ik(j)}^{n+\frac{1}{2}}$  by solving

$$\begin{aligned} L(\phi_{(j),n}^{n+1}) &= \int_0^L \bar{\rho} \frac{\mathbf{v}^{n+1} - \mathbf{v}^n}{\Delta t} \cdot \mathbf{p} dS + \int_0^L I_{22}^\rho \frac{\dot{\mathbf{d}}_1^{n+1} \cdot \mathbf{g}_1^{n+1} - \dot{\mathbf{d}}_1^n \cdot \mathbf{g}_1^n}{\Delta t} dS + \int_0^L I_{11}^\rho \frac{\dot{\mathbf{d}}_2^{n+1} \cdot \mathbf{g}_2^{n+1} - \dot{\mathbf{d}}_2^n \cdot \mathbf{g}_2^n}{\Delta t} dS + \\ &+ \int_0^L EI_1 (\mathbf{d}_3'^{n+\frac{1}{2}} \cdot \mathbf{g}_2^{n+\frac{1}{2}} + \mathbf{g}_3'^{n+\frac{1}{2}} \cdot \mathbf{d}_2^{n+\frac{1}{2}}) dS + \int_0^L EI_2 (\mathbf{d}_1'^{n+\frac{1}{2}} \cdot \mathbf{g}_3^{n+\frac{1}{2}} + \mathbf{g}_1'^{n+\frac{1}{2}} \cdot \mathbf{d}_3^{n+\frac{1}{2}}) dS + \\ &+ \int_0^L GJ (\mathbf{d}_2'^{n+\frac{1}{2}} \cdot \mathbf{g}_1^{n+\frac{1}{2}} + \mathbf{g}_2'^{n+\frac{1}{2}} \cdot \mathbf{d}_1^{n+\frac{1}{2}}) dS + \int_0^L R(\mathbf{r}' - \mathbf{d}_3)^{n+\frac{1}{2}} \cdot (\mathbf{p}' - \mathbf{g}_3^{n+\frac{1}{2}}) dS + \\ &+ \sum_{i=1}^3 \sum_{j=1}^3 \int_0^L \lambda_{ik}^{n+\frac{1}{2}} (\mathbf{d}_i \mathbf{g}_k + \mathbf{d}_k \mathbf{g}_i)^{n+\frac{1}{2}} dS - \int_0^L \mathbf{f}^{n+\frac{1}{2}} \cdot \mathbf{p} dS - \sum_{\alpha=1}^2 \int_0^L \frac{\mathbf{f}^{n+1} \cdot \mathbf{g}_\alpha^{n+1} + \mathbf{f}^n \cdot \mathbf{g}_\alpha^n}{2} dS = 0 \end{aligned}$$

for a convenient choice of  $\mathbf{g}_i$  and where the notation  $()^{n+\frac{1}{2}} = \frac{()^n + ()^{n+1}}{2}$

- Step 2: Compute the residual  $R_{(j)}^{n+1}$  of the above equation and check the convergence

Computation of the  $R_{(j)}^{n+1}$  by choosing  $\mathbf{g}_i^{n+1} = \mathbf{U} \wedge \mathbf{d}_{i(j)}^{n+1}$  and  $\mathbf{g}_i^{n+\frac{1}{2}} = \mathbf{U} \wedge (\frac{\mathbf{d}_i^{n+1} + \mathbf{d}_i^n}{2})$

Check for convergence: IF  $\|R_{(j)}^{n+1}\| \leq \text{tolerance}$  then begin new time step ( $n \rightarrow n+1$ , go to step 0).

Else: continue

Here  $(j)$  denotes the iteration of the Newton-Raphson.

- Step 3: Compute tangent matrix

$$K_T = \left[ \frac{\partial^2 L}{\partial(\mathbf{r}^{n+1}, \mathbf{d}_i^{n+1})} (\mathbf{p}, \mathbf{g}_i) \right] (\bar{\mathbf{p}}, \bar{\mathbf{g}}_i)$$

$$\forall(\mathbf{p}, \mathbf{g}_i) \in dK \text{ and } \forall(\bar{\mathbf{p}}, \bar{\mathbf{g}}_k) \in dK$$

and solve the linear system  $K_T(\bar{\mathbf{U}}, \bar{\mathbf{p}}) = R_{(j)}^{n+1}$

- Step 4: Update the configuration

• Translation

$$\mathbf{r}_{(j+1)}^{n+1} = \mathbf{r}_{(j)}^{n+1} + \mathbf{p}_{(j)}^{-n+1}$$

$$\mathbf{v}_{(j+1)}^{n+1} = \mathbf{v}_{(j)}^{n+1} + \frac{2}{\Delta t} \mathbf{p}_{(j)}^{-n+1}$$

• Rotation

$$\mathbf{d}_{i(j+1)}^{n+1} = \text{Cay}(\mathbf{d}_{i(j)}^{n+1} + \mathbf{g}_{i(j)}^{-n+1})$$

$$\dot{\mathbf{d}}_{i(j+1)}^{n+1} = (I + Q)^{-1} \left\{ \frac{4}{\Delta t} (\mathbf{d}_i^{n+1} - \mathbf{d}_i^n) + (I + Q^T) \dot{\mathbf{d}}_i^n \right\}$$

where Cay denotes for the Cayley transform [Geradin (1994)] a mapping from  $\mathbb{R}^3$  to  $\text{SO}(3)$ , the special group of rotations and  $Q = (\mathbf{d}_{i(j)}^{n+1} \otimes \mathbf{d}_i^n)$ .

- Step 5: Begin new iteration;  $j \rightarrow j+1$  go to step 2.

## 5. Numerical simulation

The aforementioned numerical methodology will be now used to the analysis of the nonlinear dynamics of undersea cables assessing the main features of the formulation proposed in the present work.

Consider a cable, hanging from a floating system in one end and fixed in the other end. If  $l$  is the length of the cable, the coordinate of the point anchored in the floating system is  $S = 0$  and  $S = l$  being the coordinate of the other fixed end.

The static configuration, Figure (2), is reached due to the self-weight of the pipe. Suppose that a harmonic motion  $U(t) = U_0 \sin(\omega t)$  is imposed at the suspended end ( $S = 0$ ), in the vertical direction. This displacement is due to the action of the sea wave on the floating body. The coordinates of the ends of the cable are  $(0, 0, 0)$  and  $(8m, 0, -1m)$  respectively for the left end right ends. Physical properties are given in Table (1).

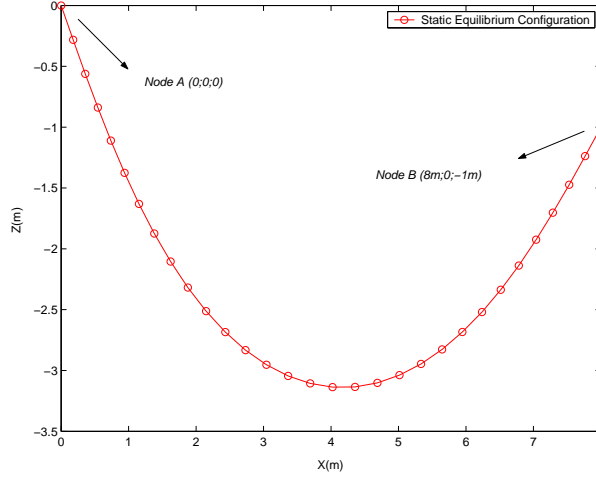


Figure 2: Static configuration.

$EA(N)$	$D(m)$	$EI(Nm^2)$	$G(Nm^2/rad)$	$l(m)$	$q(kg/m)$
$7.96 \cdot 10^8$	0.3172	$5.882 \cdot 10^4$	$9.25 \cdot 10^6$	10	226.7

Table 1: Material properties of cable.

In a first analysis, the cable is dynamically excited with a imposed frequency  $f(Hz)$  of 0.658 and an amplitude  $U_0(m)$  of 0.4, the time step is  $\Delta t = 0.1s$  and the cable is discretized by 30 finite elements. Figure (3) shows some dynamic configurations assumed by the cable after a time of excitation of 900 seconds.

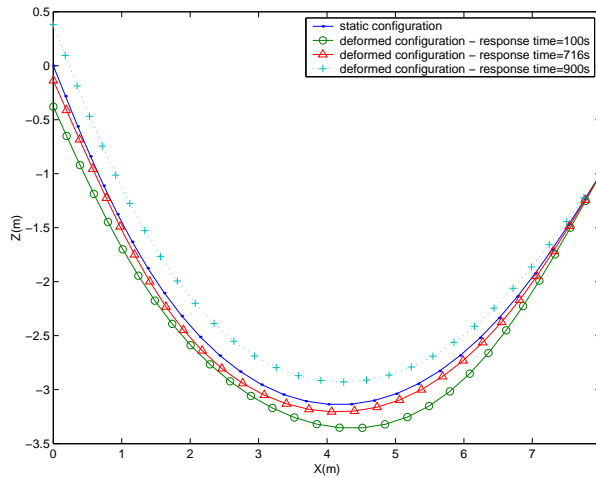


Figure 3: Dynamic configurations.

In the next case the amplitude will be kept constant and different frequencies of the imposed motion will be used. Figures (4), (5) and (6) depicts the configurations of the cable for the frequencies of 1 Hz, 1.25 Hz and 1.5 Hz respectively after a time of excitation of 15 seconds. The cable is discretized by 30 elements and the time step is of 0.015 seconds.

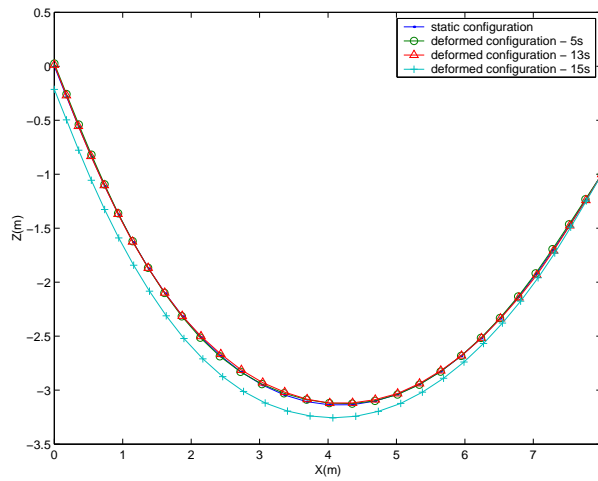


Figure 4: Dinamic configurations - frequency of 1 Hz.

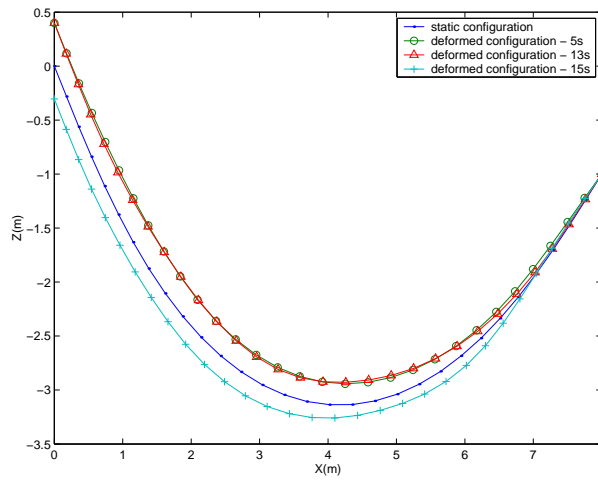


Figure 5: Dinamic configurations - frequency of 1.25 Hz.

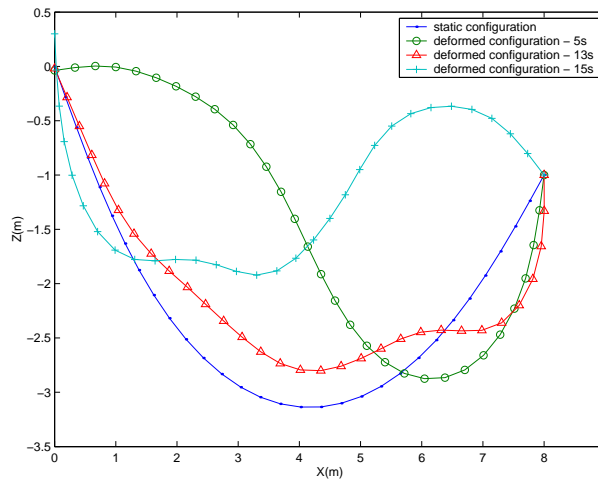


Figure 6: Dinamic configurations - frequency of 1.5 Hz.

The numerical formulation proposed is also tested for different meshes of the structure. In Table (2) the dynamic configurations are compared for the cable discretized by 10, 20 and 40 elements. The values of the coincident nodes of these meshes agree among themselves, which emphasizes the precision of the algorithm.

<i>nodes</i>	$X(m)$			$Z(m)$		
	10 elements	20 elements	40 elements	10 elements	20 elements	40 elements
2/4/8	0.55005692	0.55012231	0.55013855	-0.92118727	-0.92112472	-0.92111874
4/8/16	1.16625172	1.16626404	1.16627385	-1.70797838	-1.70792071	-1.70791546
6/12/24	1.89622038	1.89621935	1.89623243	-2.38911234	-2.38909468	-2.38908535
8/16/32	2.75582804	2.75576712	2.75579154	-2.89490232	-2.89485046	-2.89488858
10/20/40	3.71708346	3.71705769	3.71708198	-3.15826318	-3.15798844	-3.15792114
12/24/48	4.71359172	4.71349848	4.71347723	-3.14153959	-3.14137483	-3.14134350
14/28/56	5.66885119	5.66873998	5.66875000	-2.85550360	-2.85544012	-2.85537888
16/32/64	6.53205344	6.53196423	6.53194628	-2.35419700	-2.35408343	-2.35401905
18/36/72	7.29714769	7.29714531	7.29713406	-1.71140016	-1.71133363	-1.71132149

Table 2: Values of coordinates for different finite element meshes.

## 6. Conclusion

The present article has as main goal the use of a numerical formulation including a new time stepping integrator to simulate the dynamics of cables (risers or mooring lines). A numerical example (cable excited at its upper end undergoing large deformations) is verified. The results show that this algorithm achieves stable solutions combined with high precision.

## 7. References

- Antman, S.S. and Kenney, C.S., "Large Buckled States of Nonlinearly Elastic Rods under Torsion, Thrust and Gravity", *Archieve of Rational Mechanics and Analysis*, Vol. 76, pp. 289-338, 1981.
- Bailey, C.D., "Dynamics and the Calculus of Variations", *Computer Methods in Applied Mechanics and Engineering*, Vol. 60, pp. 275-287, 1987.
- Rochinha, F.A., "Modelling and Numerical Simulation of Rods", Phd Thesis-Puc Rio, 1990.
- Campos, A.D., "Non-Linear Dynamics of Rods", Phd Thesis Coppe/UFRJ, 1998.
- Galvanetto, U. and Crisfield, M.A., "An Energy-Conserving Co-Rotational Procedure for the Dynamics of Planar Beam Structures", *Int. J. for Num. Meth. in Eng.*, vol.39, pp 2265-2282, 1996.
- Geradin, M., "Application of the Finite Element Method to Dynamics of Articulated System", Internal Report, University of Liège, 1994.
- Hughes, T.J.R., "The Finite Element Method", Prentice-Hall, New Jersey, 1987.
- Aranha, J.A.P. and Pinto, M.O., "Dynamic Tension in Risers and Mooring Lines: an Algebraic Approximation for Harmonic Excitation", 2001.
- Simo, J.C. and Tarnow, N., "Non-Linear Dynamics of Three-Dimensional Rods: Exact Energy and Momentum Conserving Algorithms", *Int. Journal For Num. Meth. in Eng.*, vol. 38, pp 1431-1473, 1995.
- Simo, J. C. and Vu-quoc, L., "On The Dynamics in Space of Rods Undergoing Large Motions - A Geometrically Exact Approach", *Computer Meth. in Appl. Mech. in Eng.*, vol. 66, pp 125-161, 1988.
- Yoo, H. H., Ryan, R. R. and Scott, R. A., "Dynamics of Flexible Beams Undergoing Overall Motions", *Journal of Sound and Vibration*, vol.2., pp 261-278, 1995.
- Yazdchi M., Crisfield M.A., "Non-linear Dynamic Behaviour of Flexible Marine Pipes and Risers", *International Journal for Numerical Methods in Engineering*, 2002.

## 8. Responsibility notice

The authors are the only responsible for the printed material included in this paper.